

RESEARCH ARTICLE

Piezo channels contribute to the regulation of myelination in Schwann cells

Jenica Acheta¹ | Urja Bhatia¹ | Jeanette Haley¹ | Jiayue Hong¹ | Kyle Rich¹ | Rachel Close¹ | Marie E. Bechler^{2,3}  | Sophie Belin¹  | Yannick Poitelon¹ 

¹Department of Neuroscience and Experimental Therapeutics, Albany Medical College, Albany, New York, USA

²Department of Cell and Developmental Biology, State University of New York Upstate Medical University, Syracuse, New York, USA

³Department of Neuroscience and Physiology, State University of New York Upstate Medical University, Syracuse, New York, USA

Correspondence

Sophie Belin and Yannick Poitelon, Department of Neuroscience and Experimental Therapeutics, Albany Medical College, 47 New Scotland Avenue, MC-136, Albany, NY 12208, USA.
Email: belins@amc.edu and poitely@amc.edu

Funding information

National Institute of Neurological Disorders and Stroke, Grant/Award Number: R01 NS110627

Abstract

Peripheral nerves and Schwann cells have to sustain constant mechanical constraints, caused by developmental growth as well as stretches associated with movements of the limbs and mechanical compressions from daily activities. In Schwann cells, signaling molecules sensitive to stiffness or stretch of the extracellular matrix, such as YAP/TAZ, have been shown to be critical for Schwann cell development and peripheral nerve regeneration. YAP/TAZ have also been suggested to contribute to tumorigenesis, neuropathic pain, and inherited disorders. Yet, the role of mechanosensitive ion channels in myelinating Schwann cells is vastly unexplored. Here we comprehensively assessed the expression of mechanosensitive ion channels in Schwann cells and identified that PIEZO1 and PIEZO2 are among the most abundant mechanosensitive ion channels expressed by Schwann cells. Using classic genetic ablation studies, we show that PIEZO1 is a transient inhibitor of radial and longitudinal myelination in Schwann cells. Contrastingly, we show that PIEZO2 may be required for myelin formation, as the absence of PIEZO2 in Schwann cells delays myelin formation. We found an epistatic relationship between PIEZO1 and PIEZO2, at both the morphological and molecular levels. Finally, we show that PIEZO1 channels affect the regulation of YAP/TAZ activation in Schwann cells. Overall, we present here the first demonstration that PIEZO1 and PIEZO2 contribute to mechanosensation in Schwann cells as well myelin development in the peripheral nervous system.

KEYWORDS

Fam38a, Fam38b, myelin, PIEZO1, PIEZO2, Schwann cell

1 | INTRODUCTION

In addition to long-appreciated biochemical cues, mechanical cues in the peripheral nervous system (PNS) have emerged as major signals in nerve development, as contributors to peripheral nerve disorders (e.g., partial peripheral nerve regeneration following trauma, tumorigenesis, neuropathic pain, inherited disorders) and as targetable for non-invasive

mechanical therapies (for review, see Belin et al., 2017; Feltri et al., 2021). All cells exhibit mechanosensitivity, whereby proteins change structure, localization, or post-translational modifications in response to mechanical stimuli (pressure, stretch, shear) in the extracellular matrix (ECM) and cytoskeleton, but also following a change in extracellular stiffness or in the movement of amphipathic molecules on the lipid bilayer (for review, see Martino et al., 2018). Thus, mechanosensitive proteins have been shown to convey a range of biological responses from cell fate decisions, and cell migration to proliferation.

Jenica Acheta and Urja Bhatia contributed equally to this study.

Schwann cells, the supporting glial cells of the PNS, fulfill various roles, including trophic support of axons, facilitation of action potential conduction, and orchestration of the response to nerve injury. Schwann cells are directly sensitive to stiffness or stretch of the ECM, as demonstrated in cell culture systems (for review, see Marinval & Chew, 2021). Application of pressure in vitro promotes Schwann cell proliferation (Frieboes & Gupta, 2009). When Schwann cell cultures are subjected to stretch in vitro, YAP/TAZ, two mechanotransducers known to relay cytoskeletal tension to nuclei are activated (Poitelon et al., 2016). Schwann cells increase their proliferation and expression of nerve growth factor when subjected to tension in culture (Chen et al., 2020). Finally, Schwann cells in culture react to the ECM stiffness changes by altering their cellular morphology, motility, proliferation, and cell signaling such as the activation of YAP/TAZ (Gu et al., 2012; Lopez-Fagundo et al., 2014; Poitelon et al., 2016; Urbanski et al., 2016). Yet, besides YAP/TAZ, how Schwann cells detect, and process mechanical information is still largely unclear. In addition, the crosstalk and feedback regulation between different mechanosensitive pathways remain to be studied.

Transient receptor potential (TRP) channels are known to impart mechanosensitivity to cells (for review, see Christensen & Corey, 2007; Lin & Corey, 2005). Though it is unknown if all TRP channels are expressed in peripheral nerves and Schwann cells, several TRP channels have been shown to affect peripheral nerve repair. TRPV4 and TRPM7 regulate Schwann cell dedifferentiation following nerve injury, as ablation of either TRPV4 or TRPM7 in mouse Schwann cells impaired the demyelinating process, resulting in delayed remyelination and functional recovery of sciatic nerves (Feng et al., 2020; Kim, Lee, et al., 2020). In addition, TRPA1 mediates neuroinflammation following nerve ligation, as silencing of TRPA1 in mouse Schwann cells limited the recruitment of macrophages and allodynia (De Logu et al., 2017). Another class of mechanically activated cation channels is PIEZO channels, including PIEZO1 and PIEZO2. While these molecules were first identified to have a role predominantly in sensory tissues (important for proprioception, hearing, etc.), other roles for Piezo proteins have emerged including participation in cellular migration, proliferation, elongation, volume regulation, and cell fate (for review, see Bagriantsev et al., 2014). Recent studies have demonstrated that PIEZO1 channels also contribute to the differentiation of oligodendrocytes (Schwann cells counterparts in the central nervous system) and proliferation of oligodendrocyte precursors cells (Segel et al., 2019; Velasco-Estevez et al., 2020). Also, pharmacological inhibition of PIEZO1 in organotypic brain slices protects against demyelination (Velasco-Estevez et al., 2020). Finally, PIEZO2 was recently shown to be expressed by Schwann cells in the rat sciatic nerve (Shin et al., 2021).

Our objective in this study is to determine which mechanosensitive ion channels contribute to Schwann cell mechanosensitivity in peripheral nerves. We comprehensively investigate the expression of known mechanosensitive ion channels, including 28 TRP channels as well as PIEZO1 (encoded by *Fam38a*) and PIEZO2 (encoded by *Fam38b*) during development. Further, we demonstrate the function

of mechanosensitive ion channels PIEZO1 and PIEZO2 in Schwann cell development and PNS myelination.

To determine the contribution of Piezo-mediated mechanotransduction in Schwann cell myelination during PNS development, we generated Schwann cell-specific PIEZO1 and/or PIEZO2 conditional knockout mice (Piezo1^{CKO}, Piezo2^{CKO}, Piezo1/2^{CKO}). Further, here we identify the dysregulation of signaling pathways downstream of Piezo activation that are known to impact Schwann cell myelination. First, we show that the length and thickness of Schwann cell myelin sheaths are increased in Piezo1^{CKO} mice. In addition, using Piezo1^{CKO} mice and Yoda1-treated Schwann cells, we demonstrate that PIEZO1 activity leads to the activation of TAZ. Second, we show that in contrast to PIEZO1, Schwann cell myelination is reduced in Piezo2^{CKO} mice. Third, the absence of both channels in myelin regulation in Piezo1/2^{CKO} mimics the morphological phenotype observed in Piezo1^{CKO} with enhanced myelination and is correlated, to myelin proteins upregulation. However, the increase of myelination is independent from any modulation of YAP/TAZ, ERK, and AKT signaling pathways. In sum, our results show an epistatic relationship between PIEZO1 and PIEZO2 and a molecular association between PIEZO channels and YAP/TAZ in Schwann cells. Our study is the first to identify a molecular crosstalk between two distinct mechanosensitive pathways during the PNS development.

2 | METHODS

2.1 | Animal model

All experiments involving animals followed experimental protocols approved by the Albany Medical College Institutional Animal Care and Use Committee. Piezo1^{fl/fl} (Jackson Laboratory, #029213) and Piezo2^{fl/fl} (Jackson Laboratory, #027720) mice were derived to a congenic C57BL/6J background, bred with *Mpz-Cre* (Jackson Laboratory, #017928) used to generate Piezo1^{fl/fl}; *Mpz-Cre* (Piezo1^{CKO}), Piezo2^{fl/fl} (Piezo2^{CKO}); *Mpz-Cre*, Piezo1/2^{fl/fl}; *Mpz-Cre* (Piezo1/2^{CKO}). Genotyping of mutant mice was performed by polymerase chain reaction (PCR) on tail genomic DNA (Feltri et al., 1999; Ranade et al., 2014; Woo et al., 2014). Animals were housed in cages of 5 in 12/12-h light/dark cycles. No animals were excluded from the study. Equal numbers of males and females were included in the study. Mutant and control littermates (Piezo floxed animals without *Mpz-Cre*) from both sexes were sacrificed at 6, 15, 30, and 60 days of age, and sciatic nerves were dissected. This study was carried out in accordance with the principles of the Basel Declaration and recommendations of ARRIVE guidelines issued by the NC3Rs and approved by the Albany Medical College Institutional Animal Care and Use Committee (no. 17-08002).

2.2 | Electrophysiological analyses

Animals were analyzed 30 days of age as described previously (Poitelon et al., 2018). Mice were anesthetized with tribromoethanol,

0.4 mg/g of body weight, and placed under a heating lamp to avoid hypothermia. Motor conduction velocity of sciatic nerves were obtained with subdermal steel monopolar needle electrodes: a pair of stimulating electrodes was inserted subcutaneously near the nerve at the ankle, then at the sciatic notch, and finally at the paraspinal region at the level of the iliac crest to obtain three distinct sites of stimulation, proximal and distal, along the nerve. Electrophysiological studies comprising motor and sensory nerve conduction studies were conducted using a VikingQuest electromyography device.

2.3 | Morphological analysis

Mutant and control littermates were euthanized at the indicated ages, and sciatic nerves were dissected. Nerves were fixed in 2% buffered glutaraldehyde and post fixed in 1% osmium tetroxide. For semithin sections, after alcohol dehydration, the samples were embedded in EPON resin. Transverse sections (1 nm thick) were stained with toluidine blue and examined by light microscopy. For g ratio analysis of sciatic nerves (axon diameter/fiber diameter with outer myelin layers), semithin section images were acquired with a 100× objective. G ratios were determined for at least 100 fibers chosen randomly per animal. For internodal length, nerves were consecutively washed three times in phosphate buffer (79 mM Na₂HPO₄, 21 mM NaH₂PO₄, pH 7.4). Sciatic nerves were stained in 1% osmium, washed four times in phosphate buffer and incubated at 55°C for 12 h in 30% glycerol, followed by 12 h in 60% glycerol and 12 h in 100% glycerol (Poitelon et al., 2018). The nerves were then teased onto slides in a drop of glycerol with 27-gauge needles under a microscope. The fibers were mounted and imaged at 40× with a Zeiss microscope. Internodal lengths and corresponding fiber diameters were determined for at least 30 internodes chosen randomly per animal. For all morphological assessments, at least three animals per genotype were analyzed. Data were analyzed using ImageJ Software (<http://imagej.nih.gov/ij>) (Schneider et al., 2012).

2.4 | Schwann cell culture

Primary rat Schwann cells were produced as described (Poitelon & Feltri, 2018) and grown with DMEM supplemented with 4 g/L glucose, 2 mM L-glutamine, 5% bovine growth serum, 2 μM forskolin, 50 ng/ml nerve growth factor, penicillin and streptomycin. Schwann cells were not used beyond the fourth passage. Rat dorsal root ganglia (DRG) neurons from Sprague–Dawley rat embryos were isolated at embryonic day 14.5 embryos. DRG were dissociated by treatment with 0.25% trypsin and mechanical trituration and 1.5 DRGs were seeded on collagen-coated glass coverslips as described (Poitelon & Feltri, 2018). For GsMTx-4 (Alomone, STG-100) treatment, GsMTx-4 was solubilized in DMEM at 100 nM, then Schwann cells were treated with either DMEM or 100 μM of GsMTx-4 for 48 h (Bae et al., 2011). For Yoda-1 (Tocris, 5586) treatment, Yoda-1 was solubilized in DMSO at 1 mM, then

Schwann cells were treated with either 0.5% of DMSO or 5 μM of Yoda-1 for up to 1 h (Lacroix et al., 2018).

2.5 | Western blotting

Sciatic nerves were then frozen in liquid nitrogen, pulverized, and resuspended in lysis buffer (150 mM NaCl, 25 mM HEPES, 0.3% CHAPS, pH 7.4, 1 mM Na₃VO₄, 1 mM NaF and 1:100 Protease Inhibitor Cocktail [Roche Diagnostic, Florham Park, NJ]) (Belin, Ornaghi, et al., 2019). Protein lysates were centrifuged at 15,000g for 30 min at 4°C. Supernatant protein concentrations were determined by bicinchoninic acid assay protein assay (Thermo Scientific, Waltham, MA) according to the manufacturer's instructions. Equal amounts of homogenates were diluted 3:1 in 4× Laemmli (250 mM Tris-HCl, pH 6.8, 8% sodium dodecyl sulfate, 8% β-mercaptoethanol, 40% glycerol, 0.02% bromophenol Blue), denatured 5 min at 100°C, resolved on a SDS-polyacrylamide gel and electro-blotted onto PVDF membrane. Blots were then blocked with 5% bovine serum albumin in 1× phosphate-buffered saline (PBS), 0.05% Tween-20 and incubated overnight with the following appropriate antibodies: anti-AKT 1/1000 (Cell Signaling, 9272), anti-phospho-AKT 1/1000 (Cell Signaling, 9271), anti-Calnexin 1/3000 (Sigma, C4731), anti-ERK 1/2 1/1000 (Cell Signaling, 9102), anti-phospho-ERK 1/2 1/1000 (Cell Signaling, 9101), anti-MBP 1/1000 (Biolegend, 836504), anti-MBP 1/1000 (Biolegend, 836504), anti-P0 1/5000 (Aves, PZO8767985), anti-PIEZO1 1/200 (ProteinTech, 15939-1-AP), anti-PIEZO2 1/400 (ProSci, 8613), anti-PMP2 1/1000 (ProteinTech, 12717-1-AP), anti-TAZ 1/1000 (ProteinTech, 23306-1-AP), anti-phosphoTAZ 1/200 (Cell signaling, 59971S), anti-YAP 1/200 (Santa Cruz, sc-101199), anti-phosphoYAP 1/200 (Cell signaling, 4911S). Membranes were then rinsed in 1 X PBS and incubated for 1 h with secondary antibodies. Blots were developed using ECL or ECL plus (GE Healthcare, Chicago, IL). Western blots were quantified using Image J software (<http://imagej.nih.gov/ij>) (Poitelon et al., 2012).

2.6 | Immunohistochemistry

For nodal staining, sciatic nerves were fixed in 4% PFA and teased onto slides in a drop of PBS (Colom et al., 2012). Teased fibers were then, permeabilized with acetone, washed in PBS, blocked for 1 h in 5% fish skin gelatin, 0.5% Triton X-100 in 1× Tris-buffered saline (TBS). Primary Schwann cells and cocultures were fixed in 4% PFA, permeabilized with -20°C 100% methanol, washed in TBS, blocked for 1 h in 5% normal goat serum, 0.1% Triton in 1× TBS. The following primary antibodies were incubated overnight: anti-TAZ 1/1000 (ProteinTech, 23306-1-AP), anti-neurofilament M (Biolegend, 822701), anti-MBP 1/1000 (Biolegend, 808401), anti-Kv1.1 1/200 (Alomone labs APC-009), and anti-Pan Na 1/200 (Sigma Aldrich, S8809). Slices were washed, incubated with appropriate secondary Ab diluted in blocking solution for 1 h at room temperature, washed, stained with DAPI [1/10000] (Sigma-Aldrich, D9542) for 5 min room temperature, washed, mounted with Vectashield, then sealed. Images

were acquired with a Zeiss epifluorescent microscope. Analyses were done using Image J Software (<http://imagej.nih.gov/ij>).

2.7 | RNA preparation and real time quantitative-PCR

Sciatic nerves were dissected, stripped of epineurium, frozen in liquid nitrogen, pulverized and processed as described (Belin, Herron, et al., 2019). Total RNA was prepared from sciatic nerve or Schwann cells with TRIzol (Roche Diagnostic). One microgram of RNA was reverse transcribed using Superscript III (Invitrogen, Carlsbad, CA, United States). For each reaction, 5 μ M of oligo(dT)20 and 5 ng/ μ l random hexamers were used. Quantitative PCR was performed using the 20 ng of cDNA combined with 1 \times FastStart Universal Probe Master (Roche Diagnostic). Data were analyzed using the threshold cycle (Ct) and $2^{(-\Delta\Delta Ct)}$ method. Primer sequences for mechanosensitive

channels were obtained from previous studies (Choi et al., 2015; Maksimovic et al., 2014; Woo et al., 2014) (Data S1). *Gapdh* was used as control gene for PCR and *Rps13*, *Rps20*, *Rpl27* were used as endogenous genes of reference for real time quantitative PCR (RTq-PCR).

2.8 | Statistical analyses

Data collection and analysis were performed blind to the conditions of the experiments. Data are presented as mean \pm standard error of the mean (SEM) or standard deviation (SD). No statistical methods were used to predetermine sample sizes, but our sample sizes are based on existing literature for the respective experiments. Two-tailed Student's *t* test and two-tailed unpaired Student's *t* test with Bonferroni postdoc were used for statistical analysis of the differences between two groups. *p* values ≤ 0.05 were considered to represent a significant difference.

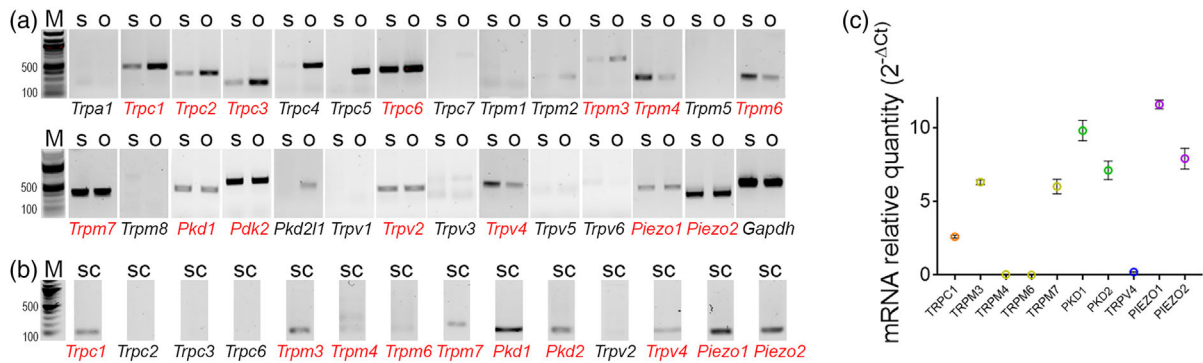


FIGURE 1 Polymerase chain reaction (PCR) and real time quantitative PCR (RTq-PCR) analysis of TRP and Piezo channels in sciatic nerves at 30 days of age and in primary Schwann cells. (a, b) Twenty-five TRP channels (1 TRPA, 7 TRPC, 8 TRPM, 3 PKD/TRPP, and 6 TRPV) and 2 PIEZO channels were examined with conventional PCR. Twenty TRP and 2 PIEZO channels were detected in sciatic nerves. Seven TRP and 2 PIEZO channels were detected in primary Schwann cells. *Gapdh* was used as a control. Genes written in red are expressed in sciatic nerves (a) or Schwann cells (b). M, DNA length marker (100 bp ladder). s, sciatic nerve. o, optic nerve. sc, Schwann cell. (c), 13 TRP channels (1 TRPC (yellow), 4 TRPM (orange), 2 PKD (green), and 1 TRPV (blue)) and 2 PIEZO (purple) channels were examined with RTq-PCR. Data represent fold differences relative to a control gene *Rps20*. *N* = 3 experiments. Data are represented in means \pm SD.

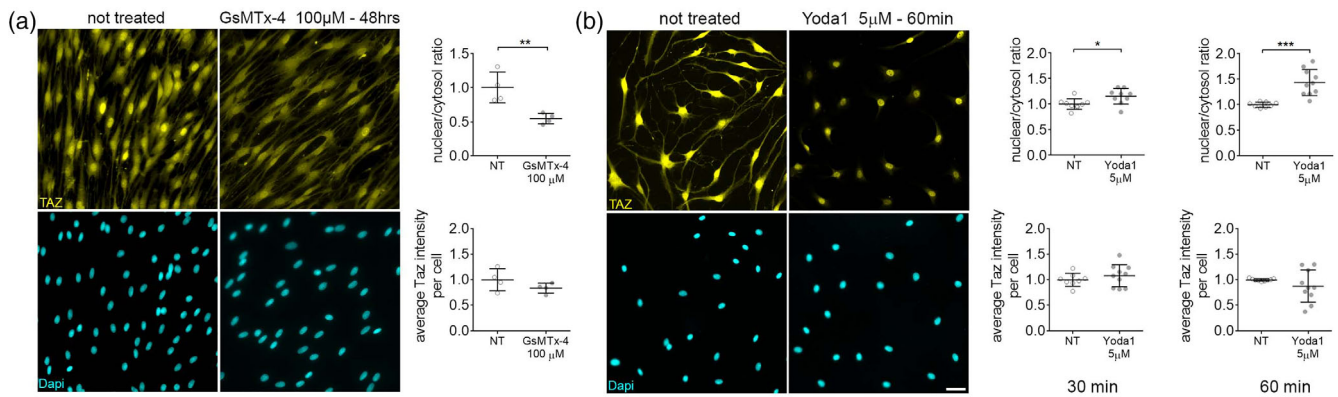


FIGURE 2 Immunofluorescence staining and quantification of the nuclear/cytoplasmic ratio of TAZ in Schwann cell cultures. (a) Schwann cells were treated with GsMTx-4 (100 μ M) for 48 h. (b) Schwann cells were starved for 12 h, then treated with Yoda1 (5 μ M) for 30 or 60 min. Cultures were stained for TAZ (yellow), and DAPI (cyan). *N* = 4–10 coverslips from three distinct experiments. Data are represented in means \pm SD. Scale bars 10 μ m. All images were acquired at the same magnification. Two-tailed unpaired Student's *t* test with Bonferroni correction. **p* value < 0.05 , ***p* value < 0.01 , ****p* value < 0.001

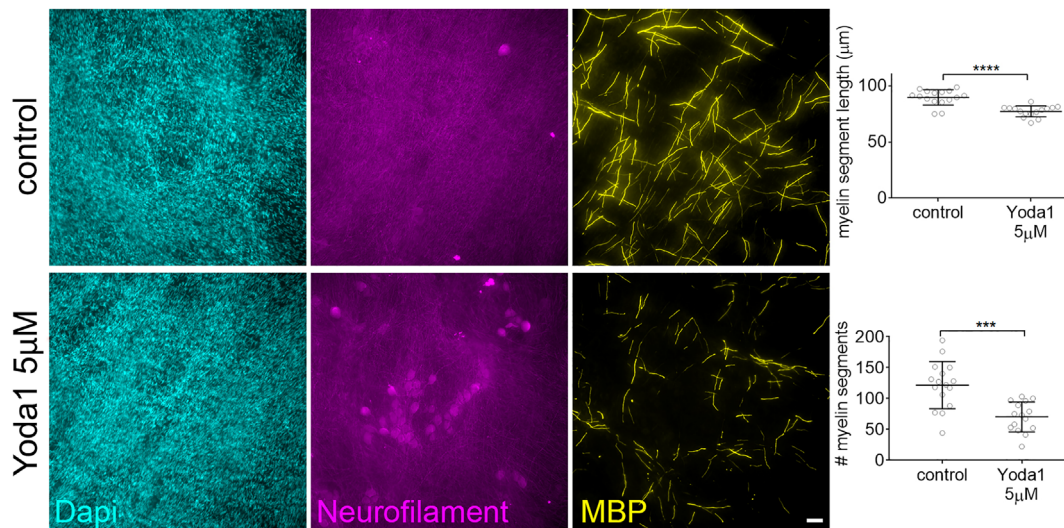


FIGURE 3 Immunofluorescence staining and quantification of the MBP segments in Schwann cell and dorsal root ganglia neuron cocultures. Cocultures were treated with ascorbic acid and Yoda1 (5 µM) for 7 days. Cocultures were stained for MBP (yellow), Neurofilament H (magenta), and DAPI (cyan). *N* = 10 coverslips from three distinct experiments. Data are represented in means ± SD. Scale bars 50 µm. All images were acquired at the same magnification. Two-tailed unpaired Student's *t* test. ****p* value <.001, *****p* value <.0001

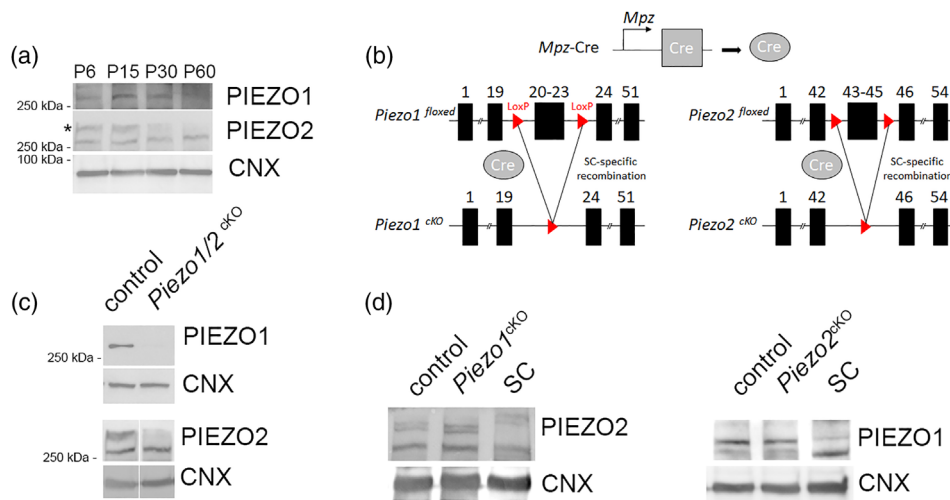


FIGURE 4 Generation and characterization of *Piezo*^{CKO} mice. (a) Western blot analysis shows that PIEZO1 and PIEZO2 protein levels are expressed in sciatic nerves. Western blot analysis was performed on C57BL/6 sciatic nerves at 6, 15, 30, and 60 days of age. *, PIEZO2 band. Also, PIEZO1 and PIEZO2 are expressed by primary rat Schwann cells (d). Calnexin was used as a protein loading control. (b) *Mpz*-Cre directed recombination in *Piezo1*^{CKO} and *Piezo2*^{CKO} mutant mice. *Mpz* activates Cre recombinase expression in Schwann cells from E13.5. Upon Cre expression, exons between LoxP sites are excised, that is, 20–23 of the *Piezo1* alleles and/or 43–45 of the *Piezo2* alleles. (c) Western blot analysis shows that PIEZO1 and PIEZO2 protein levels are decreased in sciatic nerves of *Piezo1/2*^{CKO} mice at 15 days of age. (d) Western blot analysis shows that PIEZO1 and PIEZO2 protein levels are not increased in *Piezo2*^{CKO} and *Piezo1*^{CKO} mice, respectively, at 15 days of age. Calnexin was used as a protein loading control

3 | RESULTS

3.1 | Mechanosensitive channels are expressed in Schwann cells

Recent single-cell RNA-seq papers have identified that mechanosensitive channels are expressed in peripheral nerves, mainly by fibroblast-like epineurial, perineurial, and endoneurial cells as well as endothelial cells (Chen et al., 2021; Gerber et al., 2021). Yet, no

studies have targeted which mechanosensitive channels were expressed in mouse peripheral nerves using a non-bulk RNA approach, which increase the unbiased coverage of low quantify of mRNA detection. We evaluated all the mechanosensitive isoforms for the TRP channel subfamilies expressed in vertebrates TRPA, TRPC, TRPM, TRPP, and TRPV and the two PIEZO channel isoforms in the sciatic nerve of adult C57BL/6 mice at 30 days of age. Optic nerves, which express most of TRP channels, were used as positive controls (Choi et al., 2015). Sciatic nerves expressed

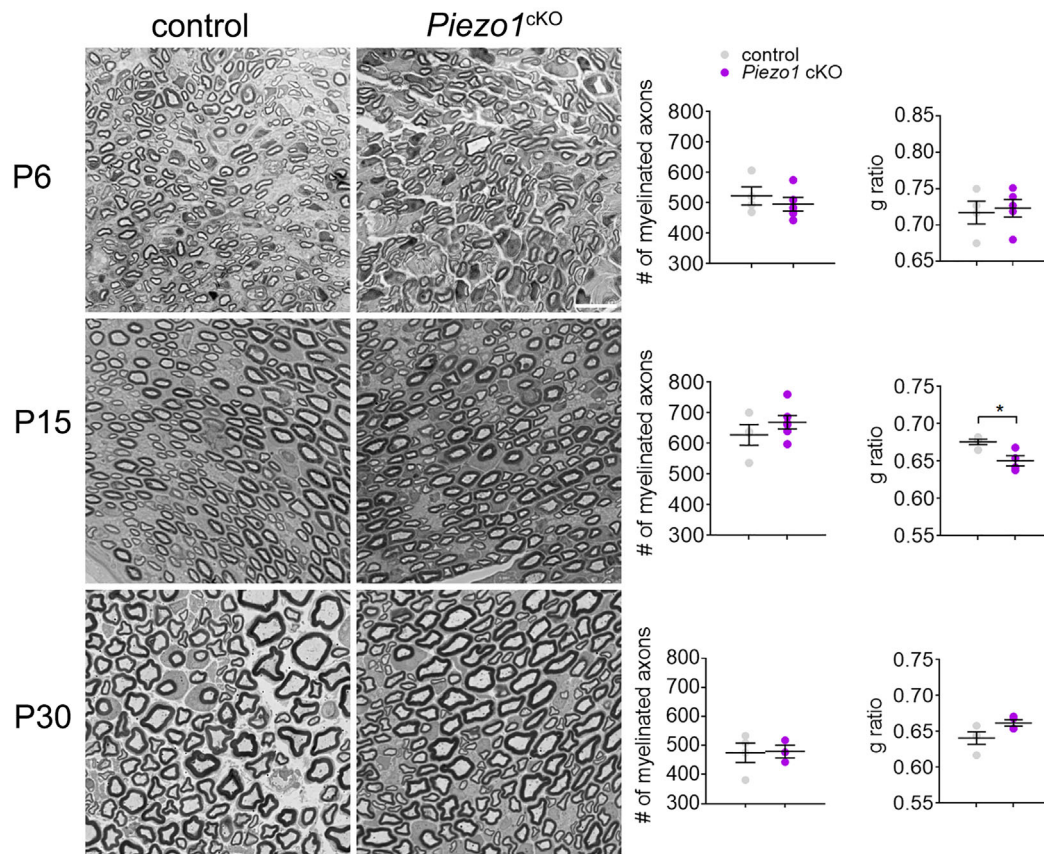


FIGURE 5 Myelination in *Piezo1*^{cKO} mice. Semithin analysis of control and *Piezo1*^{cKO} sciatic nerves at P6, P15, and P30. The number of myelinated fibers and the thickness of myelin (g ratio) were measured. $N = 3-4$ animals per genotype. Data are represented in means \pm SEM. Scale bars 10 μ m. All images were acquired at the same magnification. Two-tailed unpaired Student's *t* test. **p* value $< .05$

Trpa1, all TRPC channels (except *Trpc5* and *Trpc7*), all TRPM channels (except *Trpm5*), *Pkd1* (also known as *Trpp1*) and *Pkd2* (also known as *Trpp2*), all TRPV channels (except *Trpv1*), and both PIEZO1 and PIEZO2 channels (Figure 1a). We next determined which of the channels expressed in sciatic nerves were specifically expressed by Schwann cells. Because *Trpa1*, *Trpm1*, *Trpm2*, *Trpm8*, *Trpv3*, *Trpv5*, and *Trpv6* mRNAs were very low in sciatic nerves (Figure 1a), they were not further examined. Our conventional PCR data demonstrated that in vitro primary rat Schwann cells do not express *Trpc2*, *Trpc3*, *Trpc4*, *Trpc6*, and *Trpv2*, those isoforms might instead be expressed in the axon or by surrounding cells in the sciatic nerves (Figure 1b). However, our real-time quantitative PCR confirmed that in vitro rat Schwann cells express high level of *Trpc1*, *Trpm3*, *Trpm7*, *Pkd1*, *Pkd2*, *Piezo1*, *Piezo2* and low level of *Trpm4*, *trpm6*, and *Trpv4* (Figure 1c). The relative expression of all mechanosensitive ion channel isoforms was normalized to the housekeeping gene *Rps20*. Our data show that *Piezo1* ($2^{-\Delta Ct}$: 11.57 ± 0.3), *Pkd1* (9.8 ± 0.7), *Piezo2* (7.9 ± 0.71), and *Pkd2* (7.1 ± 0.63) among the most abundant mechanosensitive ion channel expressed by Schwann cells at 30 days of age. Similar results were obtained when compared to other housekeeping genes *Rpl27* and *Rps13* (data not shown).

3.2 | PIEZO1 regulates YAP/TAZ and myelination in Schwann cells

Pathak et al. showed that activation of PIEZO1 triggers the Ca^{2+} influx as well as the activation of transcriptional coactivator YAP in neural stem cells (Pathak et al., 2014). Given the importance of YAP/TAZ for Schwann cell and peripheral nerve development (Deng et al., 2017; Fernando et al., 2016; Grove et al., 2017; Lopez-Anido et al., 2016; Poitelon et al., 2016), we evaluated if modulation of PIEZO activity modulates YAP/TAZ activation. Schwann cell cultures were treated either with GsMTx4 peptide, a selective inhibitor of cationic mechanosensitive ion channels (e.g., PIEZO channels) or with Yoda1, a specific activator of PIEZO1. In low cell density conditions, YAP/TAZ were enriched in the Schwann cell nuclei (Figure 2a) as described previously (Poitelon et al., 2016). Blocking mechanosensitive channel activation with GsMTx4 reduced TAZ nuclear/cytosolic ratio, with a clear reduction of TAZ nuclear localization compared to untreated Schwann cells ($-45.2\% \pm 3.8$ at 48 h) (Figure 2a). To test the effect of PIEZO1 overactivation on YAP/TAZ activation, we first starved Schwann cells cultures for 12 h to limit TAZ activation (Figure 2b). Following treatment with Yoda1, Schwann cells showed an increase in TAZ nuclear/cytosolic ratio with a clear TAZ nuclear enrichment compared to untreated Schwann cells ($+15.3\% \pm 5.1$

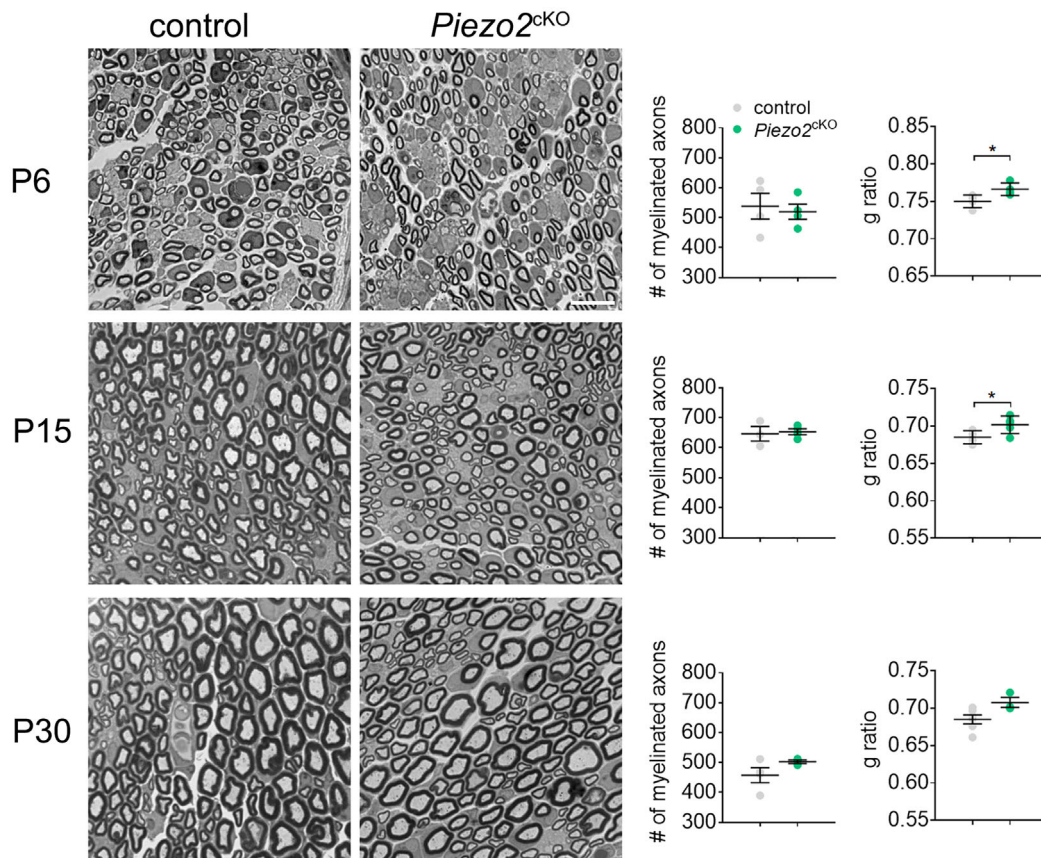


FIGURE 6 Myelination in *Piezo2^{ckO}* mice. Semithin analysis of control and *Piezo2^{ckO}* sciatic nerves at P6, P15, and P30. The number of myelinated fibers and the thickness of myelin (g ratio) were measured. $N = 4$ animals per genotype. Data are represented in means \pm SEM. Scale bars 10 μ m. All images were acquired at the same magnification. Two-tailed unpaired Student's t test. * p value $< .05$

at 30 min and $+43.3\% \pm 8.1$ at 60 min) (Figure 2b). Altogether these data suggest that PIEZO1 contribute to the activation of TAZ in Schwann cells in vitro. Unfortunately, there is no reported agonist for PIEZO2, thus we were not able to perform a similar analysis for PIEZO2.

We showed previously that in Schwann cell/neuron cocultures, YAP/TAZ were found in the nuclei of many Schwann cells. Yet, the presence of YAP/TAZ in the nuclei of myelinating Schwann cell was reduced compared to non-myelinating Schwann cells (Poitelon et al., 2016). Together with our observations here that PIEZO1 activation in culture modulates YAP/TAZ activation, this prompts the question of whether PIEZO1 activity contributes to myelin formation. We treated Schwann cell and dorsal root neurons cocultures with Yoda-1 in myelinating conditions and analyzed resulting myelin segments after 7 days. Our data show that cocultures treated with Yoda1 present both less (70.2 ± 6.3) and shorter ($77.2 \mu\text{m} \pm 1.3$) myelin segments compare to untreated cocultures ($121.6 \mu\text{m} \pm 9.5$ and $89.6 \mu\text{m} \pm 1.3$, respectively) (Figure 3).

3.3 | Conditional knock-out of Piezo channels in Schwann cells in vivo

To assess the in vivo contribution of Piezo channels to PNS myelination, we first verified the timing of PIEZO1 and PIEZO2 expression.

Prior single cell RNA-seq analysis indicated that PIEZO1 expression peaked during radial sorting at embryonic day 17.5, or during the onset of myelination at postnatal day 1 (P1) for PIEZO2 (Gerber et al., 2021). We found that in developing sciatic nerves PIEZO1 and PIEZO2 protein levels are both elevated between P6 and P15, when Schwann cells proliferate, sort axons and myelinate (Figure 4a). PIEZO1 is also expressed between P15 and P30, during growth and maturation of myelin sheaths (Figure 4a). We tried numerous approaches to localize PIEZO1 and PIEZO2 in sciatic nerve through immunohistochemistry of cross sections or teased fibers (as described in Shin et al., 2021; Velasco-Estevez et al., 2020; Zhang et al., 2019). Unfortunately, none of the commercially available Piezo antibodies was specific for immunolocalization experiments when used in *Piezo1/2^{ckO}* knockout mouse model (negative control). We also performed a Western blot for PIEZO1 and PIEZO2 in isolated Schwann cells (Figure 4d). While we do observe the presence of bands in Schwann cells, they are not at the exact same size than in sciatic nerves, indicating possibly different posttranslational modification when Schwann cells are cultured in vitro.

To analyze the role of the Piezo channels in Schwann cells in vivo, *Piezo1^{ckO}*, *Piezo2^{ckO}*, *Piezo1/2^{ckO}* were generated by using the Cre recombinase-LoxP system under the control of the *Mpz* gene. In these mice, *Mpz* activates Cre recombinase expression in Schwann

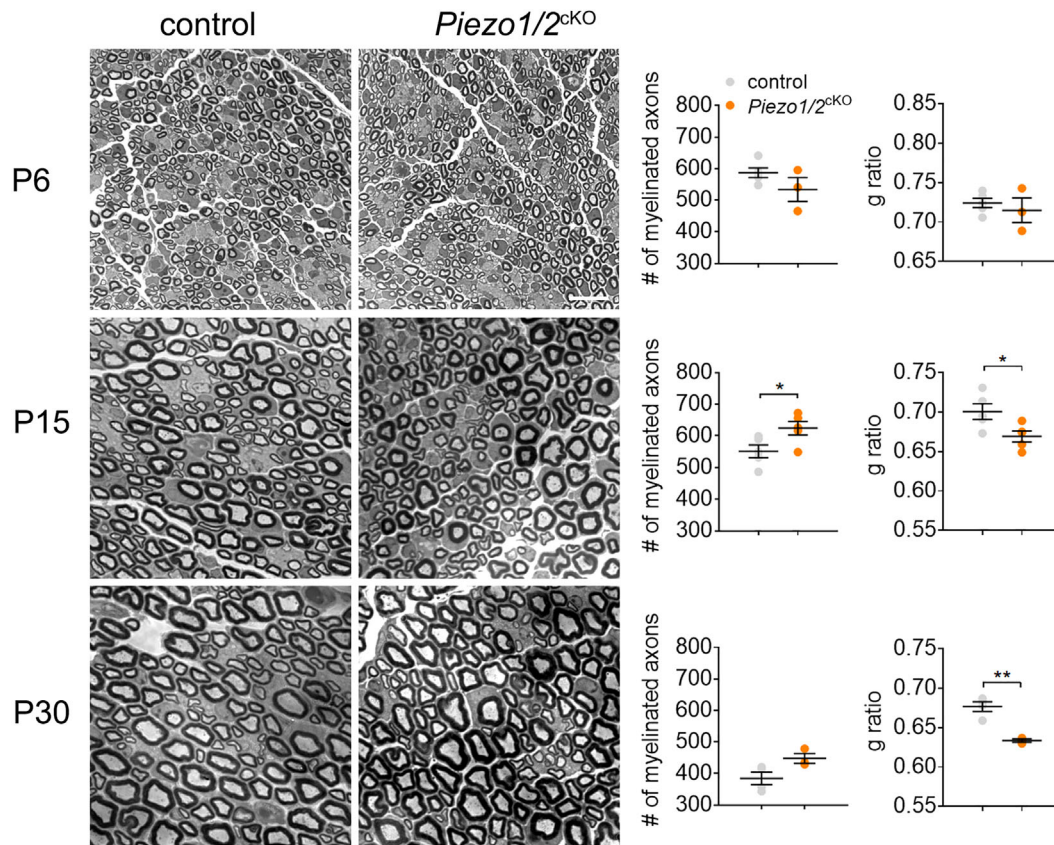


FIGURE 7 Myelination in *Piezo2*^{ckO} mice. Semithin analysis of control and *Piezo2*^{ckO} sciatic nerves at P6, P15, and P30. The number of myelinated fibers and the thickness of myelin (g ratio) were measured. $N = 3-4$ animals per genotype. Data are represented in means \pm SEM. Scale bars 10 μm . All images were acquired at the same magnification. Two-tailed unpaired Student's t test. * p value $< .05$, ** p value $< .01$

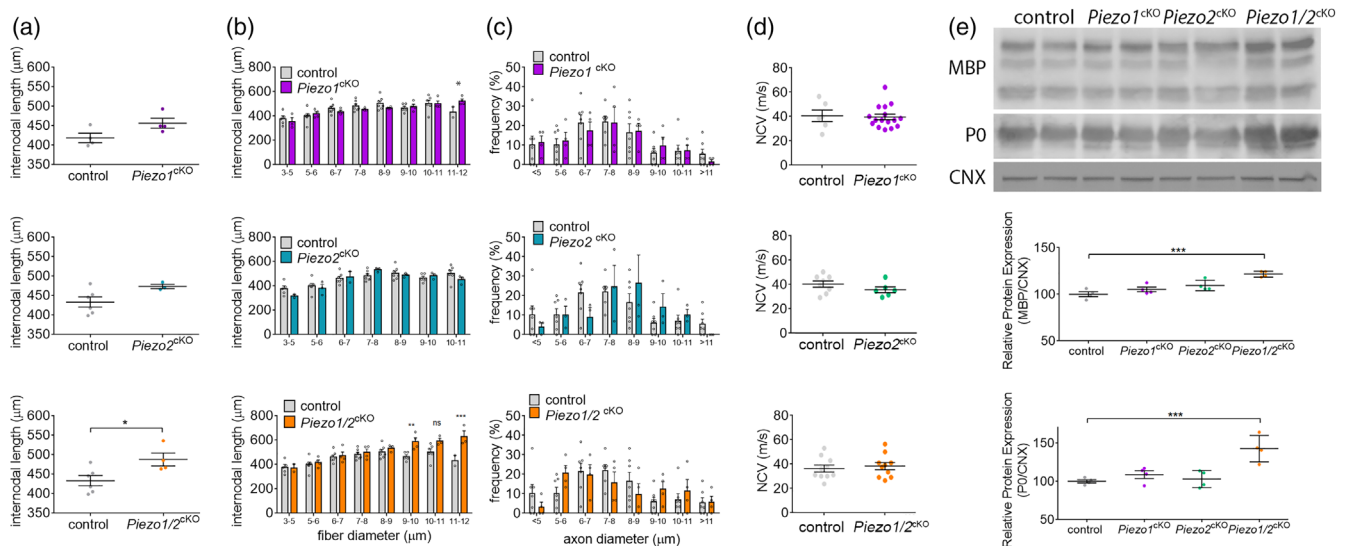


FIGURE 8 Internodal length in *Piezo*^{ckO} mice. Length of myelin internodes was measured from osmicated fibers of control and *Piezo1*^{ckO}, *Piezo2*^{ckO}, and *Piezo1/2*^{ckO} animals at 30 days of age. $N = 3-6$ animals per genotype. Data are represented as average (a) or binned in function of fiber diameter (b). Data are represented in means \pm SEM. (c) Frequency distribution of the axon calibers used in internodal length measurement. Data are represented in means \pm SEM. (d) Nerve conduction velocity measurements of control and *Piezo1*^{ckO}, *Piezo2*^{ckO}, and *Piezo1/2*^{ckO} animals at 30 days of age. $N = 6-16$ animals per genotype. Data are represented in means \pm SEM. (e) Western blot analysis of P0, MBP, and PMP2 was performed on *Piezo*^{ckO} sciatic nerves at 15 days of age. Calnexin (CNX) was used as a protein loading control. $N = 4$ animals per genotype. Data are represented in means \pm SEM. Two-tailed unpaired Student's t test (a) and two-tailed unpaired Student's t test with Bonferroni correction (b, e). * p value $< .05$, ** p value $< .01$, *** p value $< .001$

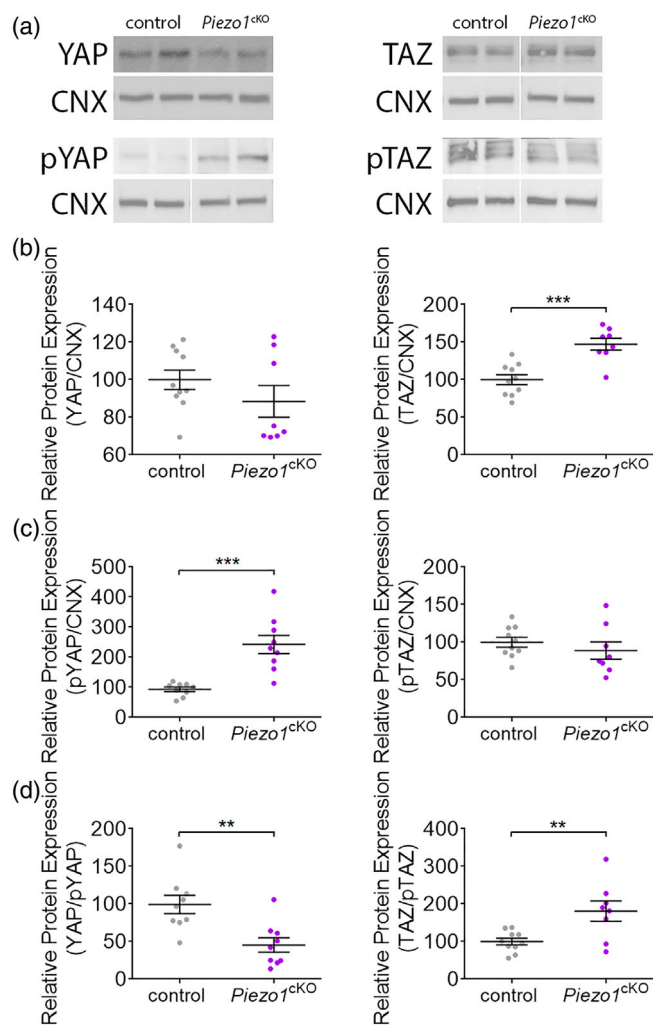


FIGURE 9 YAP/TAZ levels and phosphorylation in *Piezo1*^{CKO}. (a) Western blots analysis was performed on *Piezo1*^{CKO} sciatic nerves at 15 days of age. Calnexin (CNX) was used as a protein loading control. (b) YAP/pYAP and TAZ/pTAZ ratios are representative of YAP and TAZ activity, respectively. $N = 8-10$ animals per genotype. Data are represented in means \pm SEM. Two-tailed unpaired Student's t test. * p value $<.05$, ** p value $<.01$, *** p value $<.001$

cells at embryonic day 13.5 (E13.5) (Feltri et al., 1999). Exon 20–23 of the *Piezo1* alleles and exon 43–45 of the *Piezo2* alleles were excised during *Mpz-Cre* recombination (Ranade et al., 2014; Woo et al., 2014) (Figure 4b). Reduction of Piezo proteins level in the sciatic nerves of *Piezo1/2*^{CKO} mutant mice was verified by Western blot at postnatal day 15 (P15) (Figure 4c). PIEZO1 and PIEZO2 levels in *Piezo2*^{CKO} and *Piezo1*^{CKO} mutants were not increased, demonstrating an absence of compensation by PIEZO1 and 2, respectively (Figure 4d).

3.4 | Myelination is transiently accelerated in *Piezo1*^{CKO} and *Piezo1/2*^{CKO} sciatic nerves

To investigate the functional changes underlying the phenotype in *Piezo1*^{CKO}, *Piezo2*^{CKO}, *Piezo1/2*^{CKO} mice, ultrastructure of mutant

sciatic nerves was compared with control sciatic nerves by semithin sections at different developmental stages. At P6, *Piezo1*^{CKO} axons are properly sorted and the number of myelinated fibers is comparable to control sciatic nerves. No unmyelinated axons or myelin abnormalities were observed in *Piezo1*^{CKO} (Figure 5) at P6. At P15, the myelin was thicker in *Piezo1*^{CKO} (0.65 ± 0.007) compared to control mice (0.676 ± 0.004) (Figure 5). However, the absence of PIEZO1 has only a transient effect on early myelination, and no morphological differences were observed at P30 (Figure 5). Contrastingly, at P6 and P15, axons in *Piezo2*^{CKO} mice (P6: 0.75 ± 0.004 , P15: 0.702 ± 0.005) were transiently hypomyelinated compared to control mice (P6: 0.75 ± 0.004 , P15: 0.685 ± 0.004) (Figures 6 and S1). Finally, we examined *Piezo1/2*^{CKO} sciatic nerves (Figure 7). Similarly to *Piezo1*^{CKO}, *Piezo1/2*^{CKO} present a transient increase in the myelin thickness (P15: 0.669 ± 0.007 , P30: 0.634 ± 0.002) compared to control mice (P15: 0.701 ± 0.01 , P30: 0.677 ± 0.006) as well as an increase in the number of myelinated fibers (P15: $+13.2\% \pm 3.8$) (Figure 7). The increase in the myelin thickness seen at P15 and P30 in *Piezo1/2*^{CKO} was no longer observed at P60 (Figure S1).

We further characterized of the role of Piezo channels in Schwann cell myelination, by analyzing internodal length and node of Ranvier organization. While the average internodal length was not significantly affected by the ablation of PIEZO1 or PIEZO2 in Schwann cells (Figure 8a), internodes from fibers of large calibers were significantly longer in *Piezo1*^{CKO} (fiber of 11–12 μm : $+91.1 \mu\text{m} \pm 38.4$) (Figure 8b). The average internodal length in *Piezo1/2*^{CKO} was significantly increased ($+54.5 \mu\text{m} \pm 20.9$), especially in fibers of large calibers (fiber of 9–10 μm : $+123.4 \mu\text{m} \pm 34.6$, fiber of 11–12 μm : $+197.9 \mu\text{m} \pm 47.1$) (Figure 8b). Correlating with the increase in internodal length, we also observed an increase in MBP and PO myelin protein levels in *Piezo1/2*^{CKO} ($+21.6\% \pm 1.6$ and $+42.6\% \pm 8.6$, respectively) (Figure 8e). Finally, while changes in myelin thickness, in internodal length of large calibers fibers and nodal organization are observed in PIEZO mutants the resulting nerve conduction velocity is not affected at P30 (Figure 8d).

Because the internodal length was altered by the absence of Piezo channels in Schwann cells, we investigated the organization of Nav and Kv channels at the nodes of Ranvier. While absence of PIEZO channels did not affect the organization of Nav channels at the node of Ranvier or Kv channels at the heminode, we observed that in *Piezo1*^{CKO} ($-14.6\% \pm 2.4$) and *Piezo1/2*^{CKO} ($-19.6\% \pm 2.8$) mutants Kv channel intensity was reduced compared to control animals (Figure S2). Overall, these results indicate that PIEZO1 is an inhibitor of longitudinal myelination of large axon calibers, which might lead to a mild alteration of the quantity of Kv channels in heminodes.

Overall, these results indicate that PIEZO1 is a transient inhibitor of myelination. Our data also suggest that PIEZO2 may be required for proper myelin thickening early during development. Finally, because *Piezo1/2*^{CKO} phenotype is different from the sum of *Piezo1*^{CKO} and *Piezo2*^{CKO}, our data suggest an epistatic relationship between the two Piezo channels function in Schwann cells during myelination. A possible model for this epistatic relationship, based on the phenotype of our animal mutants, involves PIEZO2 being a promyelinating

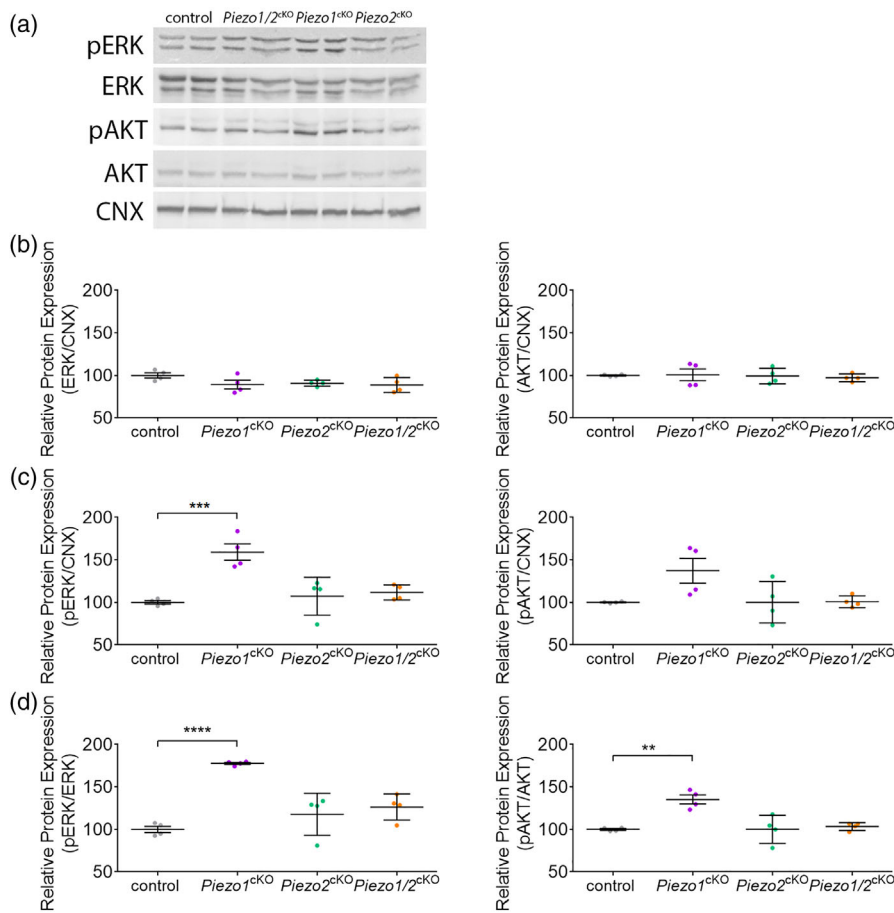


FIGURE 10 ERK and AKT levels and phosphorylation in *Piezo*^{ckO} mice. (a) Western blots analysis was performed on *Piezo*^{ckO} sciatic nerves at 15 days of age. Calnexin (CNX) was used as a protein loading control. (b) pERK/ERK and pAKT/AKT ratios are representative of ERK and AKT activity, respectively. $N = 4$ animals per genotype. Data are represented in means \pm SEM. Two-tailed unpaired Student's t test with Bonferroni postdoc test. ** p value $< .01$, *** p value $< .001$, **** p value $< .0001$

regulator and PIEZO1 being an inhibitor of PIEZO2 in the process of developmental myelination.

3.5 | YAP, TAZ, ERK, and AKT activities are altered in *Piezo1*^{ckO} sciatic nerves

Our in vitro results indicate that PIEZO1 may regulate YAP/TAZ activity in Schwann cells, and YAP/TAZ have a well characterized role in regulating Schwann cell development and myelination (Deng et al., 2017; Grove et al., 2017; Poytelon et al., 2016). At P15, when morphological differences in Piezo mutants are observed, YAP and TAZ are highly expressed in peripheral nerves (Deng et al., 2017; Poytelon et al., 2016). Therefore, we investigated YAP/TAZ levels and phosphorylation in *Piezo1*^{ckO} mutant sciatic nerves at P15, when we found the peak of expression of PIEZO1 and PIEZO2 channels in mouse sciatic nerves (Figure 4). We showed that in absence of PIEZO1, YAP activity was reduced (YAP/pYAP ratio $-53.9.6\% \pm 15.6$), while TAZ activity was increased (TAZ/pTAZ ratio $+80.9\% \pm 26.1$) (Figure 9). We also determined that while some genes known to be YAP/TAZ targets such as *Cyp61*, *Ctgf* or *Egr2* expression were unchanged (Figure S3), the increase in myelination and increase in TAZ activity observed in *Piezo1*^{ckO} correlated with the activation of signaling pathways necessary for Schwann cell myelination, that is, PI3K/AKT and mitogen-activated protein kinase (MAPK)/ERK

pathways (Maurel & Salzer, 2000; Newbern et al., 2011; Ogata et al., 2004). The activity of both ERK and AKT was increased in *Piezo1*^{ckO} P15 sciatic nerves ($+77.7\% \pm 2.4$ and $+35.2\% \pm 10.6$, respectively) (Figure 10). These results are in agreement with findings that upregulation of MAPK/ERK signaling in Schwann cells increases myelination (Belin, Ornaghi, et al., 2019; Ishii et al., 2013; Shean et al., 2014). Surprisingly, the combined absence of PIEZO1 and PIEZO2 in *Piezo1/2*^{ckO} did not affect YAP, TAZ, ERK, and AKT phosphorylation (Figures 10 and S4). Overall, these data suggest that ablation of PIEZO1 increases TAZ, ERK and AKT activities. However, since we did not observe similar dysregulation in *Piezo1/2*^{ckO}, they are unlikely to be solely causal to the effect of Piezo channels on myelination.

4 | DISCUSSION

Piezos are cation channels directly gated by mechanical forces. While activation of Piezo channels generates non-selective currents for cations such as Na^+ , K^+ , Ca^{2+} , and Mg^{2+} , both PIEZO1 and PIEZO2 are notably characterized for their role in regulating Ca^{2+} transients and Ca^{2+} signaling pathways (for review, see Parpaite & Coste, 2017). Ca^{2+} activity has been observed in myelinating cells in the central nervous system (CNS) (Baraban et al., 2018; Battefeld et al., 2019; Micu et al., 2016; Wake et al., 2011) as well as in Schwann cells in the PNS

(Heredia et al., 2018; Ino et al., 2015; Lev-Ram & Ellisman, 1995; Mayer et al., 1998; Stevens & Fields, 2000). In addition, Ca^{2+} transients, mediated by other mechanosensitive ion channels, have been shown to be altered in or causal to peripheral neuropathies (Landourey et al., 2010; Sidoli et al., 2021; Sun et al., 2019; Vanoye et al., 2019). Here, we show that Schwann cells express PIEZO1 and PIEZO2 channels and that their loss promotes or delays myelin formation, respectively, suggesting that disruption of Piezo-mediated Ca^{2+} transients in Schwann cells can regulate myelin formation.

In the CNS, Ca^{2+} transient frequency in oligodendrocytes is associated with the rate of longitudinal elongation of myelin internodes both during developmental myelination and during remyelination (Baraban et al., 2018; Bettefeld et al., 2019; Krasnow et al., 2018). Myelin sheaths that have high frequency Ca^{2+} transients grow more rapidly. However, myelin sheaths that have low frequency Ca^{2+} transient grow slowly and those with very high frequency Ca^{2+} transient shrink, indicating that the growth of myelin sheaths represents the 'sweet spot' of Ca^{2+} concentration in oligodendrocytes. In addition, mechanically induced Ca^{2+} transients were shown to modulate the ERK/MAPK pathway in oligodendrocytes (Kim, Adams, et al., 2020). In the PNS, disruption of Ca^{2+} transient in Schwann cells limits longitudinal and radial myelination (Ino et al., 2015), indicating that dose-dependent Ca^{2+} mechanisms observed in the CNS and oligodendrocytes may also apply to the PNS and Schwann cells. Therefore, it is possible that while PIEZO1 levels are expressed in sciatic nerves throughout developmental myelination, PIEZO1 channels are active only in newly formed myelinating Schwann cells, and the morphological phenotypes observed in the Schwann cell-*Piezo1*^{CKO} and *Piezo2*^{CKO} mouse models result from dysregulation of Piezo-mediated Ca^{2+} transients in myelinating Schwann cells.

Because PIEZO1 and PIEZO2 are known to be functionally redundant in other cell types, the contrasting phenotypes of Schwann cell conditional *Piezo1*^{CKO} and *Piezo2*^{CKO} mouse models is surprising. However, Piezo channels also differ in their biophysical properties. PIEZO2-mediated currents inactivate significantly faster than PIEZO1 currents (Coste et al., 2010). While PIEZO2 is only activated by membrane deformation, PIEZO1 is sensitive to both stretch and membrane deformation (Lee et al., 2014; Taberner et al., 2019). In addition, PIEZO1 and PIEZO2 are regulated by different mechanisms (Lacroix et al., 2018) or play different roles in other cell types of the nervous system (Coste et al., 2010; Qin et al., 2021). Multiple *Piezo2* variants exist, which confer functional differences to PIEZO2 (Szczyt et al., 2017), and these variants are expressed differentially in the cytosol or at the plasma membrane (Shin et al., 2021). It is therefore possible that PIEZO1 and PIEZO2 expression, activity and function varies in Schwann cells depending on the developmental stage of Schwann cells, the myelinating or non-myelinating lineage of Schwann cells, the axon and myelinated fiber diameter, or the complex changes occurring in the local environment of Schwann cells during the PNS development (Wolbert et al., 2020).

Our data also show that both expression and activation of YAP and TAZ are modulated by PIEZO1 channels. Pathak et al. suggested back in 2014 that activation of PIEZO1 triggers the Ca^{2+} influx as well

as the activation of transcriptional coactivator YAP in neural stem cells (Pathak et al., 2014). The possible molecular crosstalk between PIEZO1 and YAP pathways was further demonstrated by very recent studies in other cell types (e.g., mesenchymal or osteoblast progenitor cells, renal mesangial cells, and various tumor cell types) (Fu et al., 2021; Hasegawa et al., 2021; Liu et al., 2021; Zhou et al., 2020; Zhu et al., 2021). Indeed, PIEZO-dependent Ca^{2+} entry results in the modulation of YAP phosphorylation, localization and nuclear activity through the activation of MAPK pathway in a dose and time dependent manner (Fu et al., 2021; Liu et al., 2021). Thus, our data here suggests that the absence of PIEZO1-mediated Ca^{2+} transients lead to the activation of MAPK/ERK pathway as well as to the phosphorylation and inactivation of YAP. However, in absence of PIEZO2, PIEZO1-mediated Ca^{2+} transients do not lead to phosphorylation of MAPK/ERK or YAP/TAZ pathways, suggesting that PIEZO1 and PIEZO2 regulate Ca^{2+} transients differently in Schwann cells and that PIEZO1-mediated Ca^{2+} is PIEZO2 dependent. Nevertheless, in their current state, our data do not demonstrate whether the alteration of myelin formation seen in PIEZO mutants is a direct consequence of changes to either ERK/AKT or YAP/TAZ activity.

A multitude of extracellular, intracellular and non-biological stimuli can regulate YAP/TAZ transcriptional activity, through either phosphorylation, ubiquitination, degradation, or sequestration in the cytosol. In addition, despite having many similarities in their structures, functions and regulations, YAP and TAZ are not completely redundant (reviewed in Feltri et al., 2021). We previously showed that in Schwann cells, YAP is not able to compensate for TAZ ablation, while one TAZ allele prevents major myelin defect in YAP/TAZ double mutants (Jeanette et al., 2021; Poitelon et al., 2016). This indicates that TAZ has a prominent role to play in Schwann cell development and myelination. Here our data indicate that in sciatic nerves, PIEZO1 regulates YAP and TAZ expression and phosphorylation. While PIEZO1 might be necessary for YAP activation, PIEZO1 might be an inhibitor of TAZ expression. These *in vivo* data appear in contrast with our *in vitro* data on Schwann cells, where we showed that treatment with Yoda1 leads to an increase in TAZ activity. Considering the many functions of YAP/TAZ in Schwann cells (Deng et al., 2017; Grove et al., 2017; Poitelon et al., 2016), that YAP/TAZ are regulated by many canonical and non-canonical pathways (Feltri et al., 2021), and that the environmental constraints *in vitro* are very different than *in vivo* (Poitelon et al., 2016; Urbanski et al., 2016) these diverging results are not incompatible. Indeed, YAP/TAZ activation varies when Schwann cells are cultured alone or with neurons (Poitelon et al., 2016), TAZ expression is regulated negatively as myelination progresses (Deng et al., 2017; Poitelon et al., 2016), and TAZ activation does not correlate with myelination (Poitelon et al., 2016). Thus, it is possible that depending on the biological and cellular context PIEZO1 is a negative regulator for TAZ expression and a positive regulator for TAZ activity. Future work will be necessary to establish if the function of PIEZO1 as a transient inhibitor of Schwann cell radial and longitudinal myelination is mediated through the activation of YAP, the inhibition of TAZ, or a more complex combination of both.

YAP was previously demonstrated to be a positive regulator of longitudinal myelination. Indeed, knockdown of YAP reduced longitudinal myelination (Fernando et al., 2016). Similarly, our data indicate that in *Piezo1/2^{CKO}*, the increase in longitudinal myelination was correlated to an increase in YAP activity with the absence of PIEZO1 and PIEZO2. Other pathways known to regulate longitudinal myelination may be modulated by the increase of YAP activity (e.g., basal lamina, the dystroglycan complex, and the actin cytoskeleton complex) (reviewed in Tricaud, 2017).

In summary, our study provides *in vitro* and *in vivo* evidence supporting a novel pathway in which PIEZO channels regulate Schwann cell myelination, which may occur in part through MAPK/ERK and YAP/TAZ pathways. We have also established that PIEZO1 contributes to the regulation of YAP/TAZ in myelinating cells. Defects of myelination in the PNS are starting to be associated with mechanobiology in demyelinating diseases (i.e., traumatic and inherited) as well as tumors (for review, see Acheta et al., 2021; Feltri et al., 2021). Therefore, our observations may be relevant to better understand the intersection between mechanobiology and the molecular mechanisms regulating Schwann cell development, nerve pathology, and tumorigenesis.

AUTHOR CONTRIBUTIONS

Sophie Belin and Yannick Poitelon designed research, analyzed data and wrote the manuscript. Jenica Acheta, Urja Bhatia, Haley Jeanette, Kyle Rich, Rachel Close, Sophie Belin, and Yannick Poitelon performed experiments with Jiayue Hong, Helen Mangut, and Jacob Herron assistance. Marie E. Bechler critically reviewed the manuscript.

ACKNOWLEDGMENTS

This work was funded by NIH NINDS R01 NS110627 (to Yannick Poitelon).

CONFLICT OF INTEREST

The authors declare no competing financial interests.

DATA AVAILABILITY STATEMENT

The data that support the findings of this study are available from the corresponding author upon reasonable request.

ORCID

Marie E. Bechler  <https://orcid.org/0000-0002-2443-1353>

Sophie Belin  <https://orcid.org/0000-0003-2686-7318>

Yannick Poitelon  <https://orcid.org/0000-0001-9868-1569>

REFERENCES

- Acheta, J., Stephens, S. B. Z., Belin, S., & Poitelon, Y. (2021). Therapeutic low-intensity ultrasound for peripheral nerve regeneration—A Schwann cell perspective. *Frontiers in Cellular Neuroscience*, 15, 812588.
- Bae, C., Sachs, F., & Gottlieb, P. A. (2011). The mechanosensitive ion channel Piezo1 is inhibited by the peptide GsMTx4. *Biochemistry*, 50, 6295–6300.
- Bagriantsev, S. N., Gracheva, E. O., & Gallagher, P. G. (2014). Piezo proteins: Regulators of mechanosensation and other cellular processes. *The Journal of Biological Chemistry*, 289, 31673–31681.
- Baraban, M., Koudelka, S., & Lyons, D. A. (2018). Ca²⁺ activity signatures of myelin sheath formation and growth *in vivo*. *Nature Neuroscience*, 21, 19–23.
- Battefeld, A., Popovic, M. A., de Vries, S. I., & Kole, M. H. P. (2019). High-frequency microdomain Ca²⁺ transients and waves during early myelin internode remodeling. *Cell Reports*, 26(182–91), e5.
- Belin, S., Herron, J., VerPlank, J. J. S., Park, Y., Feltri, L. M., & Poitelon, Y. (2019). Corrigendum: YAP and TAZ regulate Cc2d1b and Purβ in Schwann cells. *Frontiers in Molecular Neuroscience*, 12, 256.
- Belin, S., Ornaghi, F., Shackelford, G., Wang, J., Scapin, C., Lopez-Anido, C., Silvestri, N., Robertson, N., Williamson, C., Ishii, A., Taveggia, C., Svaren, J., Bansal, R., Schwab, M. H., Nave, K., Fratta, P., D'Antonio, M., Poitelon, Y., Feltri, M. L., & Wrabetz, L. (2019). Neuregulin 1 type III improves peripheral nerve myelination in a mouse model of congenital hypomyelinating neuropathy. *Human Molecular Genetics*, 28, 1260–1273.
- Belin, S., Zuloaga, K. L., & Poitelon, Y. (2017). Influence of mechanical stimuli on Schwann cell biology. *Frontiers in Cellular Neuroscience*, 11, 347.
- Chen, B., Banton, M. C., Singh, L., Parkinson, D. B., & Dun, X. P. (2021). Single cell transcriptome data analysis defines the heterogeneity of peripheral nerve cells in homeostasis and regeneration. *Frontiers in Cellular Neuroscience*, 15, 624826.
- Chen, Y.-W., Wang, K., Ho, C.-C., Kao, C.-T., Ng, H. Y., & Shie, M.-Y. (2020). Cyclic tensile stimulation enrichment of Schwann cell-laden auxetic hydrogel scaffolds towards peripheral nerve tissue engineering. *Materials & Design*, 195, 108982.
- Choi, H. J., Sun, D., & Jakobs, T. C. (2015). Astrocytes in the optic nerve head express putative mechanosensitive channels. *Molecular Vision*, 21, 749–766.
- Christensen, A. P., & Corey, D. P. (2007). TRP channels in mechanosensation: Direct or indirect activation? *Nature Reviews. Neuroscience*, 8, 510–521.
- Colom, B., Poitelon, Y., Huang, W., Woodfin, A., Averill, S., Del Carro, U., Zambroni, D., Brain, S. D., Perretti, M., Ahluwalia, A., Priestley, J. V., Chavakis, T., Imhof, B. A., Feltri, M. L., & Nourshargh, S. (2012). Schwann cell-specific JAM-C-deficient mice reveal novel expression and functions for JAM-C in peripheral nerves. *26*, 1064–1076.
- Coste, B., Mathur, J., Schmidt, M., Earley, T. J., Ranade, S., Petrus, M. J., Dubin, A. E., & Patapoutian, A. (2010). Piezo1 and Piezo2 are essential components of distinct mechanically activated cation channels. *Science*, 330, 55–60.
- De Logu, F., Nassini, R., Materazzi, S., Carvalho Goncalves, M., Nosi, D., Rossi Degl'Innocenti, D., Marone, I. M., Ferreira, J., Li Puma, S., Benemei, S., Trevisan, G., Souza Monteiro de Araujo, D., Patacchini, R., Bunnett, N. W., & Geppetti, P. (2017). Schwann cell TRPA1 mediates neuroinflammation that sustains macrophage-dependent neuropathic pain in mice. *Nature Communications*, 8, 1887.
- Deng, Y., Wu, L. M. N., Bai, S., Zhao, C., Wang, H., Wang, J., Xu, L., Sakabe, M., Zhou, W., Xin, M., & Lu, Q. R. (2017). A reciprocal regulatory loop between TAZ/YAP and G-protein Galphas regulates Schwann cell proliferation and myelination. *Nature Communications*, 8, 15161.
- Feltri, M. L., D'Antonio, M., Previtali, S., Fasolini, M., Messing, A., & Wrabetz, L. (1999). PO-Cre transgenic mice for inactivation of adhesion molecules in Schwann cells. *Annals of the New York Academy of Sciences*, 883, 116–123.
- Feltri, M. L., Weaver, M. R., Belin, S., & Poitelon, Y. (2021). The Hippo pathway: Horizons for innovative treatments of peripheral nerve diseases. *Journal of the Peripheral Nervous System*, 26, 4–16.
- Feng, X., Takayama, Y., Ohno, N., Kanda, H., Dai, Y., Sokabe, T., & Tominaga, M. (2020). Increased TRPV4 expression in non-myelinating

- Schwann cells is associated with demyelination after sciatic nerve injury. *Communications Biology*, 3, 716.
- Fernando, R. N., Cotter, L., Perrin-Tricaud, C., Berthelot, J., Bartolami, S., Pereira, J. A., Gonzalez, S., Suter, U., & Tricaud, N. (2016). Optimal myelin elongation relies on YAP activation by axonal growth and inhibition by Crb3/Hippo pathway. *Nature Communications*, 7, 12186.
- Frieboes, L. R., & Gupta, R. (2009). An in-vitro traumatic model to evaluate the response of myelinated cultures to sustained hydrostatic compression injury. *Journal of Neurotrauma*, 26, 2245–2256.
- Fu, Y., Wan, P., Zhang, J., Li, X., Xing, J., Zou, Y., Wang, K., Peng, H., Zhu, Q., Cao, L., & Zhai, X. (2021). Targeting mechanosensitive Piezo1 alleviated renal fibrosis through p38MAPK-YAP pathway. *Frontiers in Cell and Development Biology*, 9, 741060.
- Gerber, D., Pereira, J. A., Gerber, J., Tan, G., Dimitrieva, S., Yanguéz, E., & Suter, U. (2021). Transcriptional profiling of mouse peripheral nerves to the single-cell level to build a sciatic nerve Atlas (SNAT). *eLife*, 10, e58591. <https://doi.org/10.7554/eLife.58591>.
- Grove, M., Kim, H., Santerre, M., Krupka, A. J., Han, S. B., Zhai, J., Cho, J. Y., Park, R., Harris, M., Kim, S., Sawaya, B. E., Kang, S. H., Barbe, M. F., Cho, S. H., Lemay, M. A., & Son, Y. J. (2017). YAP/TAZ initiate and maintain Schwann cell myelination. *eLife*, 6, e20982. <https://doi.org/10.7554/eLife.20982>.
- Gu, Y., Ji, Y., Zhao, Y., Liu, Y., Ding, F., Gu, X., & Yang, Y. (2012). The influence of substrate stiffness on the behavior and functions of Schwann cells in culture. *Biomaterials*, 33, 6672–6681.
- Hasegawa, K., Fujii, S., Matsumoto, S., Tajiri, Y., Kikuchi, A., & Kiyoshima, T. (2021). YAP signaling induces PIEZO1 to promote oral squamous cell carcinoma cell proliferation. *The Journal of Pathology*, 253, 80–93.
- Heredia, D. J., Feng, C. Y., Hennig, G. W., Renden, R. B., & Gould, T. W. (2018). Activity-induced Ca²⁺ signaling in perisynaptic Schwann cells of the early postnatal mouse is mediated by P2Y1 receptors and regulates muscle fatigue. *eLife*, 7, e30839. <https://doi.org/10.7554/eLife.30839>.
- Ino, D., Sagara, H., Suzuki, J., Kanemaru, K., Okubo, Y., & Iino, M. (2015). Neuronal regulation of Schwann cell mitochondrial Ca²⁺ signaling during myelination. *Cell Reports*, 12, 1951–1959.
- Ishii, A., Furusho, M., & Bansal, R. (2013). Sustained activation of ERK1/2 MAPK in oligodendrocytes and schwann cells enhances myelin growth and stimulates oligodendrocyte progenitor expansion. *The Journal of Neuroscience*, 33, 175–186.
- Jeanette, H., Marziali, L. N., Bhatia, U., Hellman, A., Herron, J., Kopec, A. M., Feltri, M. L., Poitelon, Y., & Belin, S. (2021). YAP and TAZ regulate Schwann cell proliferation and differentiation during peripheral nerve regeneration. *Glia*, 69, 1061–1074.
- Kim, J., Adams, A. A., Gokina, P., Zambrano, B., Jayakumaran, J., Dobrowolski, R., Maurel, P., Pfister, B. J., & Kim, H. A. (2020). Mechanical stretch induces myelin protein loss in oligodendrocytes by activating Erk1/2 in a calcium-dependent manner. *Glia*, 68, 2070–2085.
- Kim, Y. H., Lee, S., Yang, H., Chun, Y. L., Kim, D., Yeo, S. G., Park, C., Jung, J., & Huh, Y. (2020). Inhibition of transient receptor potential melastatin 7 (TRPM7) protects against Schwann cell trans-differentiation and proliferation during Wallerian degeneration. *Animal Cells and Systems (Seoul)*, 24, 189–196.
- Krasnow, A. M., Ford, M. C., Valdivia, L. E., Wilson, S. W., & Attwell, D. (2018). Regulation of developing myelin sheath elongation by oligodendrocyte calcium transients in vivo. *Nature Neuroscience*, 21, 24–28.
- Lacroix, J. J., Botello-Smith, W. M., & Luo, Y. (2018). Probing the gating mechanism of the mechanosensitive channel Piezo1 with the small molecule Yoda1. *Nature Communications*, 9, 2029.
- Landouere, G., Zdebik, A. A., Martinez, T. L., Burnett, B. G., Stanescu, H. C., Inada, H., Shi, Y., Taye, A. A., Kong, L., Munns, C. H., Choo, S. S., Phelps, C. B., Paudel, R., Houlden, H., Ludlow, C. L., Caterina, M. J., Gaudet, R., Kleta, R., Fischbeck, K. H., & Sumner, C. J. (2010). Mutations in TRPV4 cause Charcot-Marie-Tooth disease type 2C. *Nature Genetics*, 42, 170–174.
- Lee, W., Leddy, H. A., Chen, Y., Lee, S. H., Zelenski, N. A., McNulty, A. L., Wu, J., Beicker, K. N., Coles, J., Zauscher, S., Grandl, J., Sachs, F., Guilak, F., & Liedtke, W. B. (2014). Synergy between Piezo1 and Piezo2 channels confers high-strain mechanosensitivity to articular cartilage. *Proceedings of the National Academy of Sciences of the United States of America*, 111, E5114–E5122.
- Lev-Ram, V., & Ellisman, M. H. (1995). Axonal activation-induced calcium transients in myelinating Schwann cells, sources, and mechanisms. *The Journal of Neuroscience*, 15, 2628–2637.
- Lin, S. Y., & Corey, D. P. (2005). TRP channels in mechanosensation. *Current Opinion in Neurobiology*, 15, 350–357.
- Liu, S., Xu, X., Fang, Z., Ning, Y., Deng, B., Pan, X., He, Y., Yang, Z., Huang, K., & Li, J. (2021). Piezo1 impairs hepatocellular tumor growth via deregulation of the MAPK-mediated YAP signaling pathway. *Cell Calcium*, 95, 102367.
- Lopez-Anido, C., Poitelon, Y., Gopinath, C., Moran, J. J., Ma, K. H., Law, W. D., Antonellis, A., Feltri, M. L., & Svaren, J. (2016). Tead1 regulates the expression of peripheral myelin protein 22 during Schwann cell development. *Human Molecular Genetics*, 25, ddd158–ddd3069.
- Lopez-Fagundo, C., Bar-Kochba, E., Livi, L. L., Hoffman-Kim, D., & Franck, C. (2014). Three-dimensional traction forces of Schwann cells on compliant substrates. *Journal of the Royal Society Interface*, 11, 20140247.
- Maksimovic, S., Nakatani, M., Baba, Y., Nelson, A. M., Marshall, K. L., Wellnitz, S. A., Firozi, P., Woo, S. H., Ranade, S., Patapoutian, A., & Lumpkin, E. A. (2014). Epidermal Merkel cells are mechanosensory cells that tune mammalian touch receptors. *Nature*, 509, 617–621.
- Marinval, N., & Chew, S. Y. (2021). Mechanotransduction assays for neural regeneration strategies: A focus on glial cells. *APL Bioengineering*, 5, 021505.
- Martino, F., Perestrello, A. R., Vinarsky, V., Pagliari, S., & Forte, G. (2018). Cellular mechanotransduction: From tension to function. *Frontiers in Physiology*, 9, 824.
- Maurel, P., & Salzer, J. L. (2000). Axonal regulation of Schwann cell proliferation and survival and the initial events of myelination requires PI 3-kinase activity. *The Journal of Neuroscience*, 20, 4635–4645.
- Mayer, C., Quasthoff, S., & Grafe, P. (1998). Differences in the sensitivity to purinergic stimulation of myelinating and non-myelinating Schwann cells in peripheral human and rat nerve. *Glia*, 23, 374–382.
- Micu, I., Plemel, J. R., Lachance, C., Proft, J., Jansen, A. J., Cummins, K., van Minnen, J., & Stys, P. K. (2016). The molecular physiology of the axo-myelinic synapse. *Experimental Neurology*, 276, 41–50.
- Newbern, J. M., Li, X., Shoemaker, S. E., Zhou, J., Zhong, J., Wu, Y., Bonder, D., Hollenback, S., Coppola, G., Geschwind, D. H., Landreth, G. E., & Snider, W. D. (2011). Specific functions for ERK/MAPK signaling during PNS development. *Neuron*, 69, 91–105.
- Ogata, T., Iijima, S., Hoshikawa, S., Miura, T., Yamamoto, S., Oda, H., Nakamura, K., & Tanaka, S. (2004). Opposing extracellular signal-regulated kinase and Akt pathways control Schwann cell myelination. *The Journal of Neuroscience*, 24, 6724–6732.
- Parpate, T., & Coste, B. (2017). Piezo channels. *Current Biology*, 27, R250–R252.
- Pathak, M. M., Nourse, J. L., Tran, T., Hwe, J., Arulmoli, J., Le, D. T., Bernardis, E., Flanagan, L. A., & Tombola, F. (2014). Stretch-activated ion channel Piezo1 directs lineage choice in human neural stem cells. *Proceedings of the National Academy of Sciences of the United States of America*, 111, 16148–16153.
- Poitelon, Y., & Feltri, M. L. (2018). The pseudopod system for axon-glia interactions: Stimulation and isolation of Schwann cell protrusions that form in response to axonal membranes. *Methods in Molecular Biology*, 1739, 233–253.
- Poitelon, Y., Kozlov, S., Devaux, J., Vallat, J. M., Jamon, M., Roubertoux, P., Rabarimeriarijaona, S., Baudot, C., Hamadouche, T., Stewart, C. L.,



- Levy, N., & Delague, V. (2012). Behavioral and molecular exploration of the AR-CMT2A mouse model Lmna (R298C/R298C). *Neuromolecular Medicine*, 14, 40–52.
- Poitelon, Y., Lopez-Anido, C., Catignas, K., Berti, C., Palmisano, M., Williamson, C., Ameroso, D., Abiko, K., Hwang, Y., Gregorieff, A., Wrana, J. L., Asmani, M., Zhao, R., Sim, F. J., Wrabetz, L., Svaren, J., & Feltri, M. L. (2016). YAP and TAZ control peripheral myelination and the expression of laminin receptors in Schwann cells. *Nature Neuroscience*, 19, 879–887.
- Poitelon, Y., Matafora, V., Silvestri, N., Zambroni, D., McGarry, C., Serghany, N., Rush, T., Vizzuso, D., Court, F. A., Bachi, A., Wrabetz, L., & Feltri, M. L. (2018). A dual role for integrin alpha6beta4 in modulating hereditary neuropathy with liability to pressure palsies. *Journal of Neurochemistry*, 145, 245–257.
- Qin, L., He, T., Chen, S., Yang, D., Yi, W., Cao, H., & Xiao, G. (2021). Roles of mechanosensitive channel Piezo1/2 proteins in skeleton and other tissues. *Bone Research*, 9, 44.
- Ranade, S. S., Qiu, Z., Woo, S. H., Hur, S. S., Murthy, S. E., Cahalan, S. M., Xu, J., Mathur, J., Bandell, M., Coste, B., Li, Y. S., Chien, S., & Patapoutian, A. (2014). Piezo1, a mechanically activated ion channel, is required for vascular development in mice. *Proceedings of the National Academy of Sciences of the United States of America*, 111, 10347–10352.
- Schneider, C. A., Rasband, W. S., & Eliceiri, K. W. (2012). NIH image to ImageJ: 25 years of image analysis. *Nature Methods*, 9, 671–675.
- Segel, M., Neumann, B., Hill, M. F. E., Weber, I. P., Viscomi, C., Zhao, C., Young, A., Agley, C. C., Thompson, A. J., Gonzalez, G. A., Sharma, A., Holmqvist, S., Rowitch, D. H., Franze, K., Franklin, R. J. M., & Chalut, K. J. (2019). Niche stiffness underlies the ageing of central nervous system progenitor cells. *Nature*, 573, 130–134.
- Sheean, M. E., McShane, E., Cheret, C., Walcher, J., Müller, T., Wulf-Goldenberg, A., Hoelper, S., Garratt, A. N., Krüger, M., Rajewsky, K., Meijer, D., Birchmeier, W., Lewin, G. R., Selbach, M., & Birchmeier, C. (2014). Activation of MAPK overrides the termination of myelin growth and replaces Nrg1/ErbB3 signals during Schwann cell development and myelination. *Genes & Development*, 28, 290–303.
- Shin, S. M., Moehring, F., Itson-Zoske, B., Fan, F., Stucky, C. L., Hogan, Q. H., & Yu, H. (2021). Piezo2 mechanosensitive ion channel is located to sensory neurons and nonneuronal cells in rat peripheral sensory pathway: Implications in pain. *Pain*, 162, 2750–2768.
- Sidoli, M., Reed, C. B., Scapin, C., Paez, P., Cavener, D. R., Kaufman, R. J., D'Antonio, M., Feltri, M. L., & Wrabetz, L. (2021). Calcineurin activity is increased in Charcot-Marie-Tooth 1B demyelinating neuropathy. *The Journal of Neuroscience*, 41, 4536–4548.
- Stevens, B., & Fields, R. D. (2000). Response of Schwann cells to action potentials in development. *Science*, 287, 2267–2271.
- Sun, S. C., Ma, D., Li, M. Y., Zhang, R. X., Huang, C., Huang, H. J., Xie, Y. Z., Wang, Z. J., Liu, J., Cai, D. C., Liu, C. X., Yang, Q., Bao, F. X., Gong, X. L., Li, J. R., Hui, Z., Wei, X. F., Zhong, J. M., Zhou, W. J., ... Xu, X. M. (2019). Mutations in C1orf194, encoding a calcium regulator, cause dominant Charcot-Marie-Tooth disease. *Brain*, 142, 2215–2229.
- Szczot, M., Pogorzala, L. A., Solinski, H. J., Young, L., Yee, P., Le Pichon, C. E., Chesler, A. T., & Hoon, M. A. (2017). Cell-type-specific splicing of Piezo2 regulates mechanotransduction. *Cell Reports*, 21, 2760–2771.
- Taberner, F. J., Prato, V., Schaefer, I., Schrenk-Siemens, K., Heppenstall, P. A., & Lechner, S. G. (2019). Structure-guided examination of the mechanogating mechanism of PIEZO2. *Proceedings of the National Academy of Sciences of the United States of America*, 116, 14260–14269.
- Tricaud, N. (2017). Myelinating Schwann cell polarity and mechanically-driven myelin sheath elongation. *Frontiers in Cellular Neuroscience*, 11, 414.
- Urbanski, M. M., Kingsbury, L., Moussouros, D., Kassim, I., Mehjabeen, S., Paknejad, N., & Melendez-Vasquez, C. V. (2016). Myelinating glia differentiation is regulated by extracellular matrix elasticity. *Scientific Reports*, 6, 33751.
- Vanoye, C. G., Sakakura, M., Follis, R. M., Trevisan, A. J., Narayan, M., Li, J., Sanders, C. R., & Carter, B. D. (2019). Peripheral myelin protein 22 modulates store-operated calcium channel activity, providing insights into Charcot-Marie-Tooth disease etiology. *The Journal of Biological Chemistry*, 294, 12054–12065.
- Velasco-Estevez, M., Gadalla, K. K. E., Linan-Barba, N., Cobb, S., Dev, K. K., & Sheridan, G. K. (2020). Inhibition of Piezo1 attenuates demyelination in the central nervous system. *Glia*, 68, 356–375.
- Wake, H., Lee, P. R., & Fields, R. D. (2011). Control of local protein synthesis and initial events in myelination by action potentials. *Science*, 333, 1647–1651.
- Wolbert, J., Li, X., Heming, M., Mausberg, A. K., Akkermann, D., Frydrychowicz, C., Fledrich, R., Groeneweg, L., Schulz, C., Stettner, M., Alonso Gonzalez, N., Wiendl, H., Stassart, R., & Meyer Zu Horste, G. (2020). Redefining the heterogeneity of peripheral nerve cells in health and autoimmunity. *Proceedings of the National Academy of Sciences of the United States of America*, 117, 9466–9476.
- Woo, S. H., Ranade, S., Weyer, A. D., Dubin, A. E., Baba, Y., Qiu, Z., Petrus, M., Miyamoto, T., Reddy, K., Lumpkin, E. A., Stucky, C. L., & Patapoutian, A. (2014). Piezo2 is required for Merkel-cell mechanotransduction. *Nature*, 509, 622–626.
- Zhang, M., Wang, Y., Geng, J., Zhou, S., & Xiao, B. (2019). Mechanically activated Piezo channels mediate touch and suppress acute mechanical pain response in mice. *Cell Reports*, 26(1419–31), e4.
- Zhou, T., Gao, B., Fan, Y., Liu, Y., Feng, S., Cong, Q., Zhang, X., Zhou, Y., Yadav, P. S., Lin, J., Wu, N., Zhao, L., Huang, D., Zhou, S., Su, P., & Yang, Y. (2020). Piezo1/2 mediate mechanotransduction essential for bone formation through concerted activation of NFAT-YAP1-ss-catein. *eLife*, 9, e52779. <https://doi.org/10.7554/eLife.52779>.
- Zhu, B., Qian, W., Han, C., Bai, T., & Hou, X. (2021). Piezo 1 activation facilitates cholangiocarcinoma metastasis via Hippo/YAP signaling axis. *Molecular Therapy Nucleic Acids*, 24, 241–252.

SUPPORTING INFORMATION

Additional supporting information can be found online in the Supporting Information section at the end of this article.

How to cite this article: Acheta, J., Bhatia, U., Haley, J., Hong, J., Rich, K., Close, R., Bechler, M. E., Belin, S., & Poitelon, Y. (2022). Piezo channels contribute to the regulation of myelination in Schwann cells. *Glia*, 1–14. <https://doi.org/10.1002/glia.24251>